



# Quantification of birefringence readily measures the level of muscle damage in zebrafish

Joachim Berger\*, Tamar Sztal, Peter D. Currie

Australian Regenerative Medicine Institute, EMBL Australia, Monash University, Clayton, Australia

## ARTICLE INFO

### Article history:

Received 29 May 2012

Available online 16 June 2012

### Keywords:

Muscle

Zebrafish

Muscular dystrophy

Birefringence

## ABSTRACT

Muscular dystrophies are a group of genetic disorders that progressively weaken and degenerate muscle. Many zebrafish models for human muscular dystrophies have been generated and analysed, including dystrophin-deficient zebrafish mutants *dmd* that model Duchenne Muscular Dystrophy. Under polarised light the zebrafish muscle can be detected as a bright area in an otherwise dark background. This light effect, called birefringence, results from the diffraction of polarised light through the pseudo-crystalline array of the muscle sarcomeres. Muscle damage, as seen in zebrafish models for muscular dystrophies, can readily be detected by a reduction in the birefringence. Therefore, birefringence is a very sensitive indicator of overall muscle integrity within larval zebrafish. Unbiased documentation of the birefringence followed by densitometric measurement enables the quantification of the birefringence of zebrafish larvae. Thereby, the overall level of muscle integrity can be detected, allowing the identification and categorisation of zebrafish muscle mutants. In addition, we propose that the establish protocol can be used to analyse treatments aimed at ameliorating dystrophic zebrafish models.

© 2012 Elsevier Inc. All rights reserved.

## 1. Introduction

Muscular dystrophies (MD) are clinically and molecularly heterogeneous genetic diseases causing wasting of skeletal and cardiac muscle, severe local inflammation, and cycles of muscle regeneration and degeneration [1]. The clinical spectrum of MD symptoms is extremely broad. In severe forms, such as Duchenne MD, muscle regeneration is progressively exhausted, muscle fibre mass consequently becomes irreversibly replaced with fibrous connective and adipose tissue, which eventually leads to severe locomotor impairment and death, usually by respiratory and/or heart failure [2]. Patients suffering from Becker MD have milder symptoms, in some cases to a level that allows patients to lead an almost normal life. Interestingly, both types of MD are caused by mutations in the dystrophin (*DMD*) gene [3]: null mutations that cause loss of dystrophin function usually suffer from Duchenne MD and if the function of dystrophin is only partially lost patients are diagnosed with Becker MD.

Zebrafish models of disease are particularly valuable because their embryos develop *ex utero*, are translucent, highly manipulable, and genetically tractable. In addition to the large tool-set of

the zebrafish system, the zebrafish disease models often closely resemble the human disease [4]. Also the vast majority of the genes that are found to be involved in MD can be identified within the zebrafish genome [5]. Direct comparison of Duchenne MD symptoms to the pathology of dystrophin-deficient *dmd*<sup>ta222a</sup> zebrafish reveals the highly penetrant dystrophic phenotype of the zebrafish model and its close resemblance of the human disease [6,7]. In homozygous *dmd*<sup>ta222a/ta222a</sup> embryos, dystrophin is lost at the myotendinous junctions causing muscle detachment as detected by a reduction in birefringence, a light effect that results from the diffraction of polarised light through the pseudo-crystalline array of the muscle sarcomeres. Due to the non-invasive and readily accessibility of the birefringence in translucent zebrafish larvae, this marker for muscle integrity has been used to identify muscle mutants already early in the establishment of the zebrafish model system [7]. Earlier reports that analyse the birefringence of zebrafish larvae are based on pictures taken with standard dissecting microscopes, which is questionable as the birefringence is highly sensitive to the position of the larvae in relation to the polarising filters [8,9].

When two polarising light filters are placed on top of each other and the axes of polarisation are oriented 90° from each other, the intersection transmits very little light. This light effect can be reverted when a sample is placed between these two polarising filters that has two distinct refraction indices. This special biophysical property changes the state of polarised light and therefore the region, where this so called birefringent sample lies,

\* Corresponding author. Address: Australian Regenerative Medicine Institute, Monash University, Clayton Campus, Wellington Road, Clayton VIC 3800, Australia. Fax: +61 61 3 99029729.

E-mail address: [Joachim.Berger@Monash.edu](mailto:Joachim.Berger@Monash.edu) (J. Berger).

appears bright in an otherwise dark environment. Skeletal muscle is birefringent, as the refractive index for light parallel to the myofilaments is higher than that for polarised perpendicular to it [10]. Therefore, the birefringence is dependent not only upon the orientation of the two polarising filters but also of the orientation of the birefringent sample, i.e. the muscle of the larvae. If the angle of the fish larvae under polarised light is changed, the birefringence effect and the light properties of the fish larvae also change. Importantly, the illumination of the muscle evoked by the birefringence increases with the thickness of the muscle, enabling the detection of the level of muscle damage arising from either myofibre atrophy, detachment or thinning. Thus, to utilise birefringence in a comparative quantitative measure, a standard assay for its quantification needs to be developed.

We have developed an unbiased and automated assay to quantify the level of birefringence in individual zebrafish larvae, which in turn indicates the level of muscle integrity. To measure birefringence in an unbiased manner in living fish we have adapted an automated Abrio polarising light microscope. The unbiased pictures taken by the polarising microscope are subsequently used to quantify the light properties of the pictured zebrafish larvae. The developed quantification procedure allows the identification and categorisation of analysed Wildtype (WT) and muscle mutant larvae.

## 2. Materials and Methods

### 2.1. Zebrafish

The *dmd*<sup>ta222a</sup>, *sot* and *jam* mutant alleles were obtained from the Tübingen Stock Collection [7]. All mutant lines were maintained in TU background. Genotyping of the *dmd* embryos was accomplished as described [11]. Zebrafish breeding was approved by the Monash Animal Ethics Committee (number MAS/2009/05).

### 2.2. Taking unbiased birefringence pictures of zebrafish larvae with the Abrio polarising microscope

The two key components of the Abrio LS2.2 unit consist of two polarising filters (Cri, MA, USA). One is sitting in a fixed position between the sample and the light source and the other one, also called liquid crystal compensator (LC), is placed on the other side of the sample in the microscope base (Fig. 1C). The LC compensator changes the polarisation states as instructed by the Abrio software (version 2.2). Anaesthetised zebrafish larvae are placed on the microscope stage in a glass bottom FluoroDish (World Precision

Instruments, FL, USA). Importantly, the exposure levels are automatically adjusted by the Abrio software. The integrated software then automatically combines pictures of the zebrafish larvae and the resulting final picture shows the larvae with an averaged polarisation effect. This allows the generation of an unbiased picture of the birefringence of the larvae. The obtained birefringence pictures are saved as tiff-files and subsequently analysed for their brightness values.

### 2.3. Densitometry of the birefringence pictures

The area of the 2nd to the 21st somite of a pictured larva was selected in the software Fiji and the average grey value of the pixels in this area was measured, resulting in the mean grey value. This procedure was repeated and averaged over three times for each larva. For statistical analysis larvae from 3 clutches from independent breeding pairs were analysed for their muscle birefringence. Data are represented as means  $\pm$  SEM.

## 3. Results and Discussion

### 3.1. Establishment of a protocol for quantitative measures of birefringence

The birefringence intensity of the zebrafish muscle is dependent from the relative angle of the two polarising filter and the orientation of the larvae. To demonstrate the effect of the larva's orientation under the microscope, a 3 days post fertilisation (dpf) old zebrafish larva was pictured under polarising light conditions using a Leica stereomicroscope (Fig. 1). The birefringence provoked by the larva's muscle lights up the myofibres under polarised light (Fig. 1A). Rotation of the larva around its left–right axis, however, abolishes the birefringence (Fig. 1A'). In contrast, under the Abrio LS2.2 microscope a similar rotation of a zebrafish larva only slightly alters the birefringence as seen in the resulting pictures (Fig. 1B and B'). Importantly, the body of the zebrafish larva has a wedge shape, as the anterior somites that develop first are thicker than the caudal, later developing somites. This results in a gradient of birefringence from anterior-high to caudal-low. Therefore, only the somites 2–21 were used to measure the birefringence by densitometry (Fig. 1B and B'). The pictures taken by the Abrio microscope were analysed by densitometry three times each, resulting in brightness values of  $87 \pm 0.2$  and  $90 \pm 0.2$  for Fig. 1B and B', respectively. While the Abrio microscope works independently from the orientation of the larva around its left–right body axis (the plane of view), the minor difference in the mea-

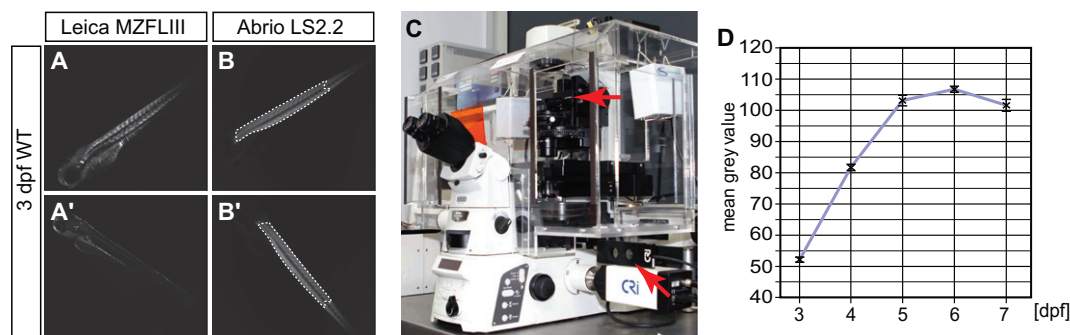


**Fig. 1.** Automation of birefringence quantification. (A) The birefringence effect illuminates the muscle of a 3 dpf old WT zebrafish larva under a Leica MZFLIII stereo microscope with polarised light conditions. (A') The birefringence effect is abolished after the larva is rotated around the left–right body axis of the larva. (B, B') In contrast, the birefringence of the encircled area of the same larva appears unaltered after a similar rotation when pictured with the Abrio LS2.2 polarising microscope. (C) The Abrio LS2.2 uses two polarising filters (arrows); the one that stays in a fixed position is placed above the object stage and the other one that is directed by the integrated software is located in the microscope base (pulled out for display purposes). (D) The birefringence of WT larvae increases during the time course from 3 dpf to 7 dpf, roughly following a sigmoid curve. Data are means  $\pm$  SEM.

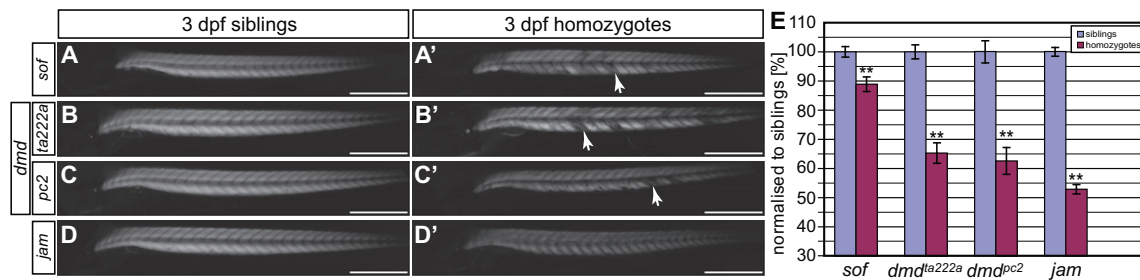


**Fig. 2.** Quantification of birefringence of zebrafish muscle mutants. (A–D) At 3 dpf the birefringence effectively visualises the muscle of the siblings larva. In comparison, the birefringence is reduced in somites with detached myofibres (arrows) in homozygous larvae of (A') *sof*, (B') *dmd<sup>ta222a</sup>*, (C') *dmd<sup>pc2</sup>*, and (D') *jam*. (E) At 3 dpf, the homozygous larvae of the muscle mutants *sof*, *dmd<sup>ta222a</sup>*, *dmd<sup>pc2</sup>*, and *jam* show a highly significant reduction in birefringence. Note the patchy appearance of the birefringence of the dystrophic muscle of *sof*, *dmd<sup>ta222a</sup>* and *dmd<sup>pc2</sup>* homozygotes that differs from the overall reduced birefringence of the *jam* mutant. Data are means ± SEM, scale bars are 0.5 mm and \*\* indicates  $P < 0.01$ .

sured birefringence probably arises from differences in the position around the anteroposterior body axis of the larva. Due to the large size and shape of the yolk sac, minor changes in the position around the anteroposterior body axis occur after larvae are repositioned. In order to account the subtle variation in measurements in subsequent experiments multiple larvae per genotype were statistically combined. In summary, the Abrio LS2.2 polarising light microscope rapidly generates an unbiased birefringence map of the fish larvae that is independent of the specimen orientation in the plane of view. Subsequent measuring of the pixel brightness allows quantification of the birefringence of zebrafish larvae.

Next, we used this established protocol to measure the birefringence of individual WT zebrafish larvae over a time course from 3 dpf to 7 dpf. As visualised in Fig. 1D, the birefringence in individual larvae increases over time, roughly following a sigmoid curve. Therefore, in subsequent experiments, the birefringence was measured at 3 dpf, which falls within the linear range of the curve. In addition, the experiment shows the importance of comparing analysed fish to control siblings of the same age, as differences in the age of the larvae will result in different birefringence measurements.

### 3.2. Analysing the birefringence of zebrafish mutants

To survey the reliability of the established procedure, we analysed the reduction of birefringence of two dystrophin-deficient zebrafish. *dmd<sup>ta222a</sup>* and *dmd<sup>pc2</sup>* harbour premature stop codons in the exons 4 and 32 of dystrophin, respectively, and are confirmed loss-of-function mutants for dystrophin [11,12]. Loss of dystrophin causes myofibre detachment followed by necrosis and death at 31 dpf in both mutants [6,12]. As the fibre detachment occurs stochastically, the somites of dystrophin-deficient larvae are differently affected, making the birefringence of these mutants appear patchy (Fig. 2B' and C'). Automated analysis of the birefringence of *dmd<sup>ta222a</sup>* and *dmd<sup>pc2</sup>* homozygotes followed by densitometry and normalisation to their siblings results in birefringence levels of  $65\% \pm 2\%$  and  $63\% \pm 4\%$  for *dmd<sup>ta222a</sup>* and *dmd<sup>pc2</sup>*, respectively (Fig. 2E). Both mutants show a highly significant reduction in birefringence when compared to their siblings ( $P < 0.01$ ,  $n = 3$ ). This calculation combines three experiments of only 7 larvae per genotype, demonstrating that the developed quantification procedure is highly reproducible. Importantly, the birefringence levels are not significantly different when homozygotes of *dmd<sup>ta222a</sup>* and *dmd<sup>pc2</sup>* are compared to each other ( $P = 0.25$ ,  $n = 3$ ). This confirms that these two mutants have a phenotype that is similar in severity, as expected from the loss of dystrophin function in both mutants [11,12].

In order to test if the quantification of the birefringence can be used to categorise the level of muscle damage in zebrafish larvae,

two additional mutants were analysed. In softy (*sof<sup>tm272a</sup>*) homozygotes muscle damage is elicited by a missense mutation in the gene *lamb2* that leads to muscle fibre detachment [13]. In contrast to dystrophin-deficient *dmd* mutants, however, detached myofibre do not undergo cell death but form ectopic myosepta [13]. Importantly, *sof* homozygotes are viable indicating that the muscle damage in *sof* is milder compared to *dmd* mutants. As a mutant with a severer muscle damage (*jam<sup>tr254a</sup>*) was chosen, an unidentified mutant that displays an equally distributed reduction in birefringence [7]. Death in *jam* homozygotes occurs at 6 dpf, much earlier than in dystrophin-deficient mutants that die at 31 dpf, indicating that *jam* is the most severely affected of the analysed mutants [7] (Fig. 2D). Quantification of the birefringence of *sof* homozygotes identifies a reduction to  $89\% \pm 2\%$  compared to their siblings. While this reduction is highly significant compared to their siblings ( $P < 0.01$ ,  $n = 3$ ), the reduction is less than in the severer affected *dmd* mutants. Homozygotes of *jam* have the highest reduction in birefringence to  $53\% \pm 2\%$ , which is compared to their siblings highly significant ( $P < 0.01$ ,  $n = 3$ ). Compared to *dmd* homozygotes that die at 31 dpf and have a reduction in birefringence to  $65\% \pm 3\%$  and  $63\% \pm 4\%$ , the birefringence seen in *jam* homozygotes that die at 6 dpf is the lowest of the analysed muscle mutants, which correlates with their severest phenotype. Similarly, *sof* homozygotes that survive to adulthood have the lowest level of reduction of birefringence to  $89\% \pm 2\%$ . This indicates that the level of reduction in birefringence in zebrafish larvae can be correlated with the level of muscle damage as indicated by the survival rate.

In summary, the developed procedure of measuring the birefringence of zebrafish larvae can be used for quantification purposes. The method produces highly reproducible results, even if only a small pool of larvae is available and can be utilised to categorise different muscle mutants, allowing comparison of the overall levels of muscle damage. Importantly, quantification of the muscle birefringence is non-invasive and readily available for the translucent zebrafish larvae. We conclude that this analysis is a valuable tool for assessing the level of muscle damage in zebrafish larvae, enabling the survey of treatments aimed at ameliorating dystrophic zebrafish models.

### Acknowledgments

We are grateful to the MMI staff for microscope maintenance and setup. JB and PDC are supported by the National Health and Medical Research Council of Australia (grant number 1024482) and the Muscular Dystrophy Association USA (grant number 201098). The Australian Regenerative Medicine Institute is supported by grants from the State Government of Victoria and the Australian Government.

## References

- [1] K.E. Davies, K.J. Nowak, Molecular mechanisms of muscular dystrophies: old and new players, *Nat. Rev. Mol. Cell Biol.* 7 (2006) 762–773.
- [2] C. Pichavant, A. Aartsma-Rus, P.R. Clemens, K.E. Davies, G. Dickson, S. Takeda, S.D. Wilton, J.A. Wolff, C.I. Wooddell, X. Xiao, J.P. Tremblay, Current status of pharmaceutical and genetic therapeutic approaches to treat DMD, *Mol. Ther.* 19 (2011) 830–840.
- [3] E.P. Hoffman, R.H. Brown Jr., L.M. Kunkel, Dystrophin: the protein product of the Duchenne muscular dystrophy locus, *Cell* 51 (1987) 919–928.
- [4] G.J. Lieschke, P.D. Currie, Animal models of human disease: zebrafish swim into view, *Nat. Rev. Genet.* 8 (2007) 353–367.
- [5] L.S. Steffen, J.R. Guyon, E.D. Vogel, R. Beltre, T.J. Pusack, Y. Zhou, L.I. Zon, L.M. Kunkel, Zebrafish orthologs of human muscular dystrophy genes, *BMC Genomics* 8 (2007) 79.
- [6] J. Berger, S. Berger, T.E. Hall, G.J. Lieschke, P.D. Currie, Dystrophin-deficient zebrafish feature aspects of the Duchenne muscular dystrophy pathology, *Neuromuscul. Disord.* 20 (2010) 826–832.
- [7] M. Granato, F.J. van Eeden, U. Schach, T. Trowe, M. Brand, M. Furutani-Seiki, P. Haffter, M. Hammerschmidt, C.P. Heisenberg, Y.J. Jiang, D.A. Kane, R.N. Kelsh, M.C. Mullins, J. Odenthal, C. Nusslein-Volhard, Genes controlling and mediating locomotion behavior of the zebrafish embryo and larva, *Development* 123 (1996) 399–413.
- [8] W.R. Telfer, A.S. Busta, C.G. Bonnemann, E.L. Feldman, J.J. Dowling, Zebrafish models of collagen VI-related myopathies, *Hum. Mol. Genet.* 19 (2010) 2433–2444.
- [9] S.M. Jacobson, D.A. Birkholz, M.L. McNamara, S.B. Bharate, K.M. George, Subacute developmental exposure of zebrafish to the organophosphate pesticide metabolite, chlorpyrifos-oxon, results in defects in Rohon-Beard sensory neuron development, *Aquat. Toxicol.* 100 (2010) 101–111.
- [10] A.F. Huxley, Looking back on muscle, in: A.L. Hodgkin (Ed.), *The Pursuit of Nature*, Cambridge University Press, Cambridge, 1977, pp. 23–64.
- [11] J. Berger, S. Berger, A.S. Jacoby, S.D. Wilton, P.D. Currie, Evaluation of exon-skipping strategies for duchenne muscular dystrophy utilizing dystrophin-deficient zebrafish, *J. Cell. Mol. Med.* (2011).
- [12] D.I. Bassett, R.J. Bryson-Richardson, D.F. Daggett, P. Gautier, D.G. Keenan, P.D. Currie, Dystrophin is required for the formation of stable muscle attachments in the zebrafish embryo, *Development* 130 (2003) 5851–5860.
- [13] A.S. Jacoby, E. Busch-Nentwich, R.J. Bryson-Richardson, T.E. Hall, J. Berger, S. Berger, C. Sonntag, C. Sachs, R. Geisler, D.L. Stemple, P.D. Currie, The zebrafish dystrophic mutant softy maintains muscle fibre viability despite basement membrane rupture and muscle detachment, *Development* 136 (2009) 3367–3376.